Dual parametrization of the proton generalized parton distribution functions H and E, and description of the deeply virtual Compton scattering cross sections and asymmetries

V. Guzey* and T. Teckentrup†

Institut für Theoretische Physik II, Ruhr-Universität Bochum, D-44780 Bochum, Germany

(Received 7 August 2006; published 21 September 2006)

We develop the minimal model of a new leading order parametrization of generalized parton distributions (GPDs) introduced by Polyakov and Shuvaev. The model for GPDs H and E is formulated in terms of the forward quark distributions, the Gegenbauer moments of the D-term, and the forward limit of the GPD E. The model is designed primarily for small and medium-size values of x_B, $x_B \leq 0.2$. We examine two different models of the t dependence of the GPDs: the factorized exponential model and the nonfactorized Regge-motivated model. Using our model, we successfully described the deeply virtual Compton scattering (DVCS) cross section measured by H1 and ZEUS, the moments of the beam-spin $A_{\mathrm{LU}}^{\sin\phi}$, the beam-charge $A_C^{\cos\phi}$, and the transversely polarized target $A_{\mathrm{UT}}^{\sin\varphi\cos\phi}$ DVCS asymmetries measured by HERMES and $A_{\mathrm{LU}}^{\sin\phi}$ measured by CLAS. The data on $A_C^{\cos\phi}$ prefer the Regge-motivated model of the t dependence of the GPDs. The data on $A_{\mathrm{UT}}^{\sin\varphi\cos\phi}$ indicate that the u and d quarks carry only a small fraction of the proton total angular momentum.

DOI: 10.1103/PhysRevD.74.054027 PACS numbers: 13.60.−r, 12.38.Lg

I. INTRODUCTION

Generalized parton distributions (GPDs) parametrize nonperturbative parton correlation functions in hadronic targets [1–7]. The GPDs generalize and interpolate between the common parton distributions and form factors. Collinear factorization theorems for deeply virtual Compton scattering [8] and for hard electroproduction of mesons [9] give a theoretical possibility to experimentally constrain the GPDs. However, since the GPDs are functions of three arguments (excluding the known dependence on the renormalization scale) and since experimental observables involve convolution of the GPDs with hard scattering coefficients and not the GPDs themselves, it is very difficult to experimentally constrain the GPDs. Therefore, there is continuing interest in modeling GPDs using various models of the hadronic structure [10–19].

The most convenient and widely used parametrization of GPDs is based on the double distribution (DD) model introduced by Radyushkin [17,18]. Adding to the DD model the so-called D-term [20], which is required to restore the full form of polynomiality of the DD model, one obtains a simple, almost analytical, parametrization of GPDs, which can be readily used for the calculation of various observables; see e.g. [4]. However, such a parametrization of the GPDs has several phenomenologically unsatisfactory features. First, the successful description of the low Bjorken x HERA data on the total deeply virtual Compton scattering (DVCS) cross section requires a very specific (ξ-independent) shape for the input GPDs, which is very different from the input required for the description of the DVCS asymmetries measured at higher x [5,21]. Second, the parametrization "does not commute" with QCD evolution, i.e. it serves only to define the input for QCD evolution of GPDs at a certain initial scale μ_0. The result of the QCD evolution to the higher scale μ cannot be generally expressed in the form used for the input. Therefore, one has to separately perform the rather nontrivial QCD evolution of GPDs. Third, the parametrization does not allow for an intuitive physical motivation and interpretation; see [22,23] for a discussion of the physics of GPDs.

In this paper, we continue and extend the analysis [24] of a new parametrization of proton GPDs first introduced by Polyakov and Shuvaev [25].

Initially, the dual representation of quark GPDs of the pion was derived by Polyakov [26] as a formal solution reproducing Mellin moments of the pion GPDs. In turn, the moments were related by crossing to the moments of the two-pion distribution amplitude, which was expanded in terms of eigenfunctions of the corresponding QCD evolution equation (the Gegenbauer polynomials $C_n^{3/2}$) and eigenfunctions of the operator of the relative orbital momentum of the pion pair (the Legendre polynomials P_l). The resulting parametrization of GPDs was termed dual because the idea of its derivation follows the hypothesis of duality of soft hadron-hadron interactions, which is the assumption that the $2 \to 2$ scattering amplitude in the s channel can be represented as an infinite series over t-channel exchanges [27]. In the context of the quark GPDs of the pion, the dual parametrization implies that the GPDs are formally given by an infinite sum of t-channel resonances, which build up the two-pion distribution amplitude.

In the successive work, Polyakov and Shuvaev postulated that a similar dual parametrization holds for proton singlet GPDs [25],

*Electronic address: vadim.guzey@tp2.rub.de
†Electronic address: tobias.teckentrup@tp2.rub.de

$$H^i(x,\xi,t,\mu^2) = \sum_{\substack{n=1\\ \text{odd}}}^{\infty}\sum_{\substack{l=0\\ \text{even}}}^{n+1} B^i_{nl}(t,\mu^2)\theta(\xi-|x|)\left(1-\frac{x^2}{\xi^2}\right) \times C_n^{3/2}\left(\frac{x}{\xi}\right)P_l\left(\frac{1}{\xi}\right),$$

$$E^i(x,\xi,t,\mu^2) = \sum_{\substack{n=1\\ \text{odd}}}^{\infty}\sum_{\substack{l=0\\ \text{even}}}^{n+1} C^i_{nl}(t,\mu^2)\theta(\xi-|x|)\left(1-\frac{x^2}{\xi^2}\right) \times C_n^{3/2}\left(\frac{x}{\xi}\right)P_l\left(\frac{1}{\xi}\right). \quad (1)$$

In this equation, the superscript i denotes the quark flavor; x, ξ, t, and μ^2 stand for the usual arguments of GPDs [4]; B^i_{nl} and C^i_{nl} denote the unknown form factors. In this work, we restrict ourselves only to the helicity-even spin-independent GPDs H and E and do not consider the two remaining helicity-even spin-dependent GPDs $\tilde{H}$ and $\tilde{E}$. Since we are concerned with DVCS observables, which probe the singlet combinations of GPDs, we shall consider only singlet GPDs: The left-hand side of Eq. (1) represents the singlet combinations of the GPDs, $H^i(x,\xi,t) \equiv H^i(x,\xi,t) - H^i(-x,\xi,t)$ and $E^i(x,\xi,t) \equiv E^i(x,\xi,t) - E^i(-x,\xi,t)$, which are antisymmetric with respect to x.

It should be stressed that the series in Eq. (1) diverges and, hence, one should explain how this should be understood. As follows from the derivation [26], Eq. (1) is nothing but a shorthand notation for the x moments of the GPDs. Therefore, the formal representation of Eq. (1) should be understood as a generalized mathematical function, which, acting on the polynomials of x, reproduces correctly the Mellin moments of the corresponding GPDs. Note that the divergence in Eq. (1) is analogous to the divergence of any dual representation of the $2 \to 2$ scattering amplitude in soft hadronic physics: The s-channel series must diverge to reproduce infinities (poles) of the amplitude in the crossed t channel [27].

Naturally, since the series in Eq. (1) diverges, one cannot use it to study the GPDs as functions of their variables. However, since Eq. (1) fixes all Mellin moments of the GPDs, one can readily obtain different representations of the GPDs, which would give continuous and finite GPDs. For instance, expanding Eq. (1) over the Gegenbauer polynomials $C_n^{3/2}(x)$ on the interval $-1 \le x \le 1$, one obtains [28]

$$H^i(x,\xi,t,\mu^2) = (1-x^2)\sum_{\substack{n=1\\ \text{odd}}}^{\infty} A^i_n(\xi,t,\mu^2)C_n^{3/2}(x), \quad (2)$$

where

$$A^i_n(\xi,t,\mu^2) = -\frac{2n+3}{(n+1)(n+2)}\sum_{\substack{p=1\\ \text{odd}}}^{n}\xi R_{np}(\xi) \times \frac{(p+1)(p+2)}{2p+3}\sum_{\substack{l=0\\ \text{even}}}^{p+1} B^i_{pl}(t,\mu^2)P_l\left(\frac{1}{\xi}\right). \quad (3)$$

The functions $R_{np}(\xi)$ are polynomials of the order n of the variable ξ, which are defined in terms of the hypergeometric function,

$$R_{np}(\xi) = (-1)^{(n+p)/2}\frac{\Gamma(\frac{3}{2}+\frac{n+p}{2})}{\Gamma(\frac{n-p}{2}+1)\Gamma(\frac{3}{2}+p)} \times \xi^p {}_2F_1\left(\frac{p}{2}-\frac{n}{2},\frac{3}{2}+\frac{n}{2}+\frac{p}{2},\frac{5}{2}+p;\xi^2\right). \quad (4)$$

The representation for the GPDs E^i is obtained by replacing the form factors B^i_{nl} by C^i_{nl}.

The dependence of the GPDs H^i and E^i on the renormalization scale μ is contained in the form factors B^i_{nl}. By construction (1), B^i_{nl} are proportional to the nth conformal moment of the GPDs, which is multiplicatively renormalized to the leading α_s accuracy [28]. Therefore, under leading order (LO) QCD evolution, the form factors B^i_{nl} have a very simple, well-established μ^2 dependence,

$$B^i_{nl}(\mu^2) = B^i_{nl}(\mu_0^2)\left(\frac{\ln(\mu_0^2/\Lambda^2)}{\ln(\mu^2/\Lambda^2)}\right)^{\gamma_n/B}, \quad (5)$$

where $B = 11 - (2/3)N_{\text{flav}}$ (N_{flav} is the number of active parton flavors); γ_n are LO nonsinglet anomalous dimensions [29,30]. Alternatively, as will be clear from the following sections, the μ^2 dependence of B^i_{nl} for all l is given by the μ^2 dependence of the $n+1$ Mellin moment of the forward singlet quark distribution, $\int_{-1}^{1} dx x^n q^i(x,\mu^2)$.

In addition to the simple LO evolution of B^i_{nl}, the DVCS amplitude has a very simple form in terms of B^i_{nl}, also only to the LO accuracy. Therefore, we shall use the dual parametrization of the GPDs as a LO parametrization.

II. MINIMAL MODEL OF THE DUAL PARAMETRIZATION OF GPDS H^i AND E^i

In this section, we consider a minimal model of the dual parametrization of the GPDs H^i and E^i, which is formulated in terms of the forward limit of the GPDs H^i and E^i and the Gegenbauer moments of the D-term. The t dependence of the GPDs is modeled separately.

A. Derivation of the minimal model

As explained in the Introduction, the dual representation in the form of Eqs. (2)–(4) gives finite and continuous expressions for GPDs H^i and E^i. However, these equations are impractical to use since one has to sum an infinite series of large sign-alternating terms. An elegant method to sum the series of Eq. (2) was offered by Polyakov and Shuvaev

[25]. The method consists of the introduction of a set of functions whose Mellin moments generate the form factors B^i_{nl} and C^i_{nl},

$$B^i_{nn+1-k}(t,\mu^2) = \int_0^1 dx x^n Q^i_k(x,t,\mu^2),$$
$$C^i_{nn+1-k}(t,\mu^2) = \int_0^1 dx x^n R^i_k(x,t,\mu^2). \quad (6)$$

Note that, for the singlet combinations of the GPDs that we consider in this paper, n is odd and k is even. Using the methods detailed in Appendix B of [25], one obtains the following representation of the GPDs H^i in terms of the generating functions Q^i_k (the GPDs E^i are obtained by replacing Q^i_k by R^i_k):

$$H^i(x,\xi,t,\mu^2) = \sum_{\substack{k=0\\ \text{even}}}^{\infty}\Bigg[\frac{\xi^k}{2}(H^{i(k)}(x,\xi,t,\mu^2) - H^{i(k)}(-x,\xi,t,\mu^2)) + \left(1-\frac{x^2}{\xi^2}\right)\theta(\xi-|x|)\sum_{\substack{l=1\\ \text{odd}}}^{k-3} C^{3/2}_{k-l-2}\left(\frac{x}{\xi}\right)P_l\left(\frac{1}{\xi}\right) \times \int_0^1 dy y^{k-l-2} Q^i_k(y,t,\mu^2)\Bigg], \quad (7)$$

where

$$H^{i(k)}(x,\xi,t,\mu^2) = \frac{1}{\pi}\int_0^1 \frac{dy}{y}\left[\left(1-y\frac{\partial}{\partial y}\right)Q^i_k(y,t,\mu^2)\right] \times \int_{-1}^1 ds \frac{x_s^{1-k}}{\sqrt{2x_s - x_s^2 - \xi^2}} \times \theta(2x_s - x_s^2 - \xi^2) - \lim_{y\to 0} Q^i_k(y,t,\mu^2) \times \int_{-1}^1 ds \frac{x_s^{1-k}}{\sqrt{2x_s - x_s^2 - \xi^2}} \times \theta(2x_s - x_s^2 - \xi^2). \quad (8)$$

Note that the term proportional to $\lim_{y\to 0} Q^i_k$ for $H^{i(k)}$ is missing in the original formulation [25]: Its presence was noticed in Ref. [31].

In the present work, we consider a minimal version of the dual representation, which consists of retaining only the contributions of the generating functions Q^i_0 and Q^i_2 to the GPDs H^i, and functions R^i_0 and R^i_2 to the GPDs E^i. This means that we keep only the form factors B^i_{nn+1}, B^i_{nn-1}, C^i_{nn+1}, and C^i_{nn-1}, i.e. we keep only the maximal $l = n+1$ and next-to-maximal $l = n-1$ orbital momenta in Eq. (1). The main motivation for such an approximation is the prefactor ξ^k in Eq. (7): In the HERA kinematics ($\xi < 0.005$), the contribution of Q^i_k and R^i_k with $k \geq 2$ is kinematically suppressed. In the HERMES kinematics ($\xi < 0.1$), we keep Q^i_2 and R^i_2 as a first correction. This is also true for the contribution of the third term in Eq. (7).

The formal representation (1) enables one to readily establish the connection between the Mellin moments of the GPDs H^i and the form factors B^i_{nl} (a similar equation holds for E^i),

$$\int_{-1}^1 dx x^N H^i(x,\xi,t,\mu^2) = \xi^{N+1}\sum_{\substack{n=1\\ \text{odd}}}^{N}\sum_{\substack{l=0\\ \text{even}}}^{n+1} B^i_{nl}(t,\mu^2)P_l\left(\frac{1}{\xi}\right) \times \frac{\Gamma(\frac{3}{2})\Gamma(N+1)(n+1)(n+2)}{2^N\Gamma(\frac{N-n}{2}+1)\Gamma(\frac{N+n}{2}+\frac{5}{2})}. \quad (9)$$

Taking the $\xi \to 0$ limit in this equation, one determines the form factors B^i_{nn+1} and C^i_{nn+1},

$$B^i_{nn+1}(t,\mu^2) = \frac{2n+3}{2n+4}\int_{-1}^1 dx x^n H^i(x,0,t,\mu^2) \equiv \frac{2n+3}{2n+4}\int_0^1 dx x^n (q^i(x,t,\mu^2) + \bar{q}^i(x,t,\mu^2)),$$
$$C^i_{nn+1}(t,\mu^2) = \frac{2n+2}{2n+4}\int_{-1}^1 dx x^n E^i(x,0,t,\mu^2) \equiv \frac{2n+3}{2n+4}\int_0^1 dx x^n (e^i(x,t,\mu^2) + \bar{e}^i(x,t,\mu^2)). \quad (10)$$

In the forward limit $t \to 0$, $q^i(x,t,\mu^2) + \bar{q}^i(x,t,\mu^2)$ become the singlet combination of forward quark parton distributions and $e^i(x,t,\mu^2) + \bar{e}^i(x,t,\mu^2)$ become the unknown forward limit of the singlet combination of GPDs E^i.

Since Eqs. (10) fix all B^i_{nn+1} and C^i_{nn+1}, they completely determine the generating functions Q^i_0 and R^i_0 [25,31],

$$Q^i_0(x,t,\mu^2) = q^i(x,t,\mu^2) + \bar{q}^i(x,t,\mu^2) - \frac{x}{2}\int_x^1 \frac{dz}{z^2}(q^i(z,t,\mu^2) + \bar{q}^i(z,t,\mu^2)),$$
$$R^i_0(x,t,\mu^2) = e^i(x,t,\mu^2) + \bar{e}^i(x,t,\mu^2) - \frac{x}{2}\int_x^1 \frac{dz}{z^2}(e^i(z,t,\mu^2) + \bar{e}^i(z,t,\mu^2)). \quad (11)$$

Therefore, up to the t dependence, the functions Q^i_0 and R^i_0 are completely constrained by the forward parton distributions and the forward limit of the GPDs E^i. Note that Eqs. (11) are valid at all scales μ^2.

Turning to the generating functions Q^i_2, we notice that their modeling is more ambiguous as compared to the functions Q^i_0 since only the Mellin moments of Q^i_2 are constrained. The constraints can be derived as follows. Considering the Mellin moments of the GPDs H^i [see Eq. (9)], we notice that the coefficient in front of ξ^{N+1}, which is denoted $h^{(N)}_{N+1}$ [4], is

$$h_{N+1}^{i(N)} = \sum_{\substack{n=1\\ \text{odd}}}^{N} \sum_{\substack{l=0\\ \text{even}}}^{n+1} B_{nl}^{i}(t,\mu^2) P_l(0) \times \frac{\Gamma(\frac{3}{2})\Gamma(N+1)(n+1)(n+2)}{2^N \Gamma(\frac{N-n}{2}+1)\Gamma(\frac{N+n}{2}+\frac{5}{2})}. \quad (12)$$

On the other hand, decomposing the D-term in terms of its Gegenbauer moments

$$D^i(z,t,\mu^2) = (1-z^2)\sum_{\substack{n=1\\ \text{odd}}}^{\infty} d_n^i(t,\mu^2) C_n^{3/2}(z) \quad (13)$$

and using the definition

$$h_{N+1}^{i(N)} = \int_{-1}^{1} dz z^N D^i(z,t,\mu^2), \quad (14)$$

one obtains the desired relation between the D-term and the form factors B_{nl}^i,

$$d_n^i(t,\mu^2) = \sum_{l=0}^{n+1} B_{nl}^i(t,\mu^2) P_l(0). \quad (15)$$

Within the framework of the minimal version of the dual parametrization, we keep only the form factors with $l = n \pm 1$ and, hence, obtain

$$B_{nn-1}^i(t,\mu^2) = \frac{n}{n+1} B_{nn+1}^i(t,\mu^2) + \frac{d_n^i(t,\mu^2)}{P_{n-1}(0)}. \quad (16)$$

This equation allows us to constrain the generating function Q_2^i as follows. Decomposing Q_2^i as

$$Q_2^i(x,t,\mu^2) = Q_0^i(x,t,\mu^2) - \int_x^1 \frac{dz}{z} Q_0^i(z,t,\mu^2) + \tilde{Q}_2^i(x,t,\mu^2) \quad (17)$$

and substituting this in Eq. (16), one obtains the following constraint on the new unknown function $\tilde{Q}_2^i$,

$$\int_0^1 dx x^n \tilde{Q}_2^i(x,t,\mu^2) = \frac{d_n^i(t,\mu^2)}{P_{n-1}(0)}. \quad (18)$$

The introduction of the functions $\tilde{Q}_2^i$ is an attempt to reduce the intrinsic theoretical uncertainty in the functions Q_2^i by separating the latter into the contribution given by the known functions Q_0^i and the contribution of the functions $\tilde{Q}_2$, whose Mellin moments are proportional to the Gegenbauer moments of the nucleon D-term.

Turning to the generating functions R_2^i for the GPDs E^i, we notice that, since the D-term contribution to the GPDs E^i and H^i are equal and opposite in sign (see e.g. [4]), then

$$C_{nn-1}^i(t,\mu^2) = \frac{n}{n+1} C_{nn+1}^i(t,\mu^2) - \frac{d_n^i(t,\mu^2)}{P_{n-1}(0)}. \quad (19)$$

Therefore, the functions R_2^i can be written in the form

$$R_2^i(x,t,\mu^2) = R_0^i(x,t,\mu^2) - \int_x^1 \frac{dz}{z} R_0^i(z,t,\mu^2) - \tilde{Q}_2^i(x,t,\mu^2). \quad (20)$$

Note that this representation for R_2^i was first suggested by Polyakov and Shuvaev; see Eq. (56) of [25].

B. Details of the minimal model

So far we have presented a rather general consideration involved in the construction of the minimal model of the dual parametrization of the GPDs H^i and E^i. In the following, we shall discuss such details of the parametrization as the modeling of the functions $\tilde{Q}_2^i$ and $e^i + \bar{e}^i$ and the modeling of the t dependence of Q_k^i and R_k^i.

In the following discussion of $\tilde{Q}_2^i$ and $e^i + \bar{e}^i$, we assume that $t = 0$ and do not explicitly write the t dependence. The shape of the functions $\tilde{Q}_2^i$ is unconstrained. We assume a simple form for $\tilde{Q}_2^i$,

$$\tilde{Q}_2^i(x,\mu^2) = (1-x)(a^i(\mu^2) + b^i(\mu^2)x + c^i(\mu^2)x^2), \quad (21)$$

with the coefficients a^i, b^i, and c^i fixed by the constraint of Eq. (18) evaluated for $n = 1$, 3, and 5. Note that the μ^2 dependence of d_n^i and, hence, the μ^2 dependence of a^i, b^i, and c^i are given by Eq. (5). In Eq. (21), we assumed that, similarly to Q_0^i, $\tilde{Q}_2^i \to 0$ in the $x \to 1$ limit and that $\tilde{Q}_2^i$ is a nonsingular polynomial in x like the nucleon D-term (13).

The singlet combination of the first three Gegenbauer moments of the D-term was evaluated in the chiral quark soliton model at the low normalization point $\mu_0 \approx 0.6$ GeV [32],

$$d_n^u(\mu_0^2) + d_n^d(\mu_0^2) = R_n[(M_2^u(\mu_0^2) + M_2^d(\mu_0^2)] = R_n, \quad R_1 = -8, \quad R_3 = -2.4, \quad R_5 = -0.8, \quad (22)$$

where M_2^i is the proton momentum fraction carried by the quark and antiquark of the flavor i. Note that the last equality in the first line of Eq. (22) comes from the fact that, at the low normalization point μ_0, in the SU(2)-symmetric chiral quark soliton model, the u and d quarks carry the entire proton momentum. At higher μ^2 of the order of a few GeV^2, the quarks carry about half of the proton momentum, which reduces the numerical values in Eq. (22) by a factor of 2 [32]. In our analysis, we use

$$d_n^u(\mu^2) = R_n M_2^u(\mu^2), \quad d_n^d(\mu^2) = R_n M_2^d(\mu^2), \quad d_n^s = 0. \quad (23)$$

Note that Eq. (23) is valid at all scales μ^2. The quark momentum fractions are evaluated using the leading order CTEQ5L parton distributions [33].

Since the GPDs E^i decouple in the forward limit, the functions $e^i + \bar{e}^i$ in Eq. (10) are unconstrained. In this work, we follow the simple model of Ref. [4], which correctly reproduces the forward limit of the first moment of the GPDs E^i and which allows us to vary the fraction of

the nucleon spin carried by quarks,

$$e^i(x,\mu^2) = A_i(\mu^2) q^i_{\rm val}(x,\mu^2) + \frac{B_i(\mu^2)}{2}\delta(x),$$
$$\bar{e}^i(x,\mu^2) = \frac{B_i(\mu^2)}{2}\delta(x), \tag{24}$$

where $q^i_{\rm val}(x,\mu^2) = q^i(x,\mu^2) - \bar{q}^i(x,\mu^2)$ is the valence quark distribution. Note that, unlike $\bar{q}^i$, $\bar{e}^i$ is a symmetric function of x. The coefficients A_i and B_i for u and d quarks are found from the first and second Mellin moments of the GPDs E^i [4],

$$A_i(\mu^2) = \frac{2J^i(\mu^2) - M_2^i(\mu^2)}{M_2^{i,\rm val}},$$
$$B_u(\mu^2) = k_u - 2A_u(\mu^2), \qquad B_d(\mu^2) = k_d - A_d(\mu^2), \tag{25}$$

where J^i is the contribution to the proton total angular momentum of the quark with flavor i; $M_2^{i,\rm val}$ is the proton momentum fraction carried by the valence part of the quark distribution function; $k_u = 1.673$ and $k_d = -2.033$ are quark anomalous magnetic moments. We assume that, for the strange and charm quarks, $e^i(x) = \bar{e}^i(x) = 0$. Note also that the μ^2 dependence of J^i is the same as for M_2^i; see e.g. [4].

In summary, the x and ξ dependence of the GPDs H^i is specified by Eqs. (11), (17), (18), and (21). The GPDs E^i are specified by Eqs. (11), (20), (24), and (25).

The t dependence of the form factors B^i_{nl} and C^i_{nl} is not known and has to be specified separately. In this work, we consider two models of the t dependence. The first model assumes that all B^i_{nl} and C^i_{nl} and, hence, H^i and E^i have a factorized exponential t dependence with the μ^2-dependent slope [24],

$$H^i(x,\xi,t,\mu^2) = \exp\left(\frac{B(\mu^2)t}{2}\right) H^i(x,\xi,t=0,\mu^2),$$
$$E^i(x,\xi,t,\mu^2) = \exp\left(\frac{B(\mu^2)t}{2}\right) E^i(x,\xi,t=0,\mu^2), \tag{26}$$

where

$$B(\mu^2) = 7.6(1 - 0.15\ln(\mu^2/2))\ \text{GeV}^2. \tag{27}$$

The decrease of the slope with increasing μ^2 was taken from the model [34]. The normalization of the slope was chosen in order to reproduce the result of the exponential fit to the t dependence of the differential DVCS cross section measured by the H1 Collaboration at HERA for $0.1 \le |t| \le 0.8$ GeV^2 and at $\mu^2 = 8$ GeV^2, $B(\mu^2 = 8\ \text{GeV}^2) = 6.02 \pm 0.35 \pm 0.39$ GeV^{-2} [35]. Note that a factorized model of the t dependence with the μ^2-independent slope commutes with the QCD evolution. While this is not so in our case (26), effects of the μ^2 dependence of the slope $B(\mu^2)$ on the QCD evolution are numerically small and, thus, have been neglected.

The second model of the t dependence is much more involved: It is nonfactorized and, hence, the t dependence nontrivially changes with QCD evolution. Since the dual parametrization of GPDs is constructed as an infinite series of t-channel exchanges, which resembles the representation of hadron-hadron scattering amplitudes in Regge theory, this analogy can serve as a guide for the t dependence of the GPDs. In particular, we use the following Regge-theory-motivated model for $q^i(t)$ and $\bar{q}^i(t)$ [4]:

$$q^i(x,t,\mu_0^2) - \bar{q}^i(x,t,\mu_0^2) = q^i_{\rm val}(x,t,\mu_0^2) = \left(\frac{1}{x^{\alpha'_{\rm val}t}}\right) q^i_{\rm val}(x,\mu_0^2),$$
$$q^i(x,t,\mu_0^2) + \bar{q}^i(x,t,\mu_0^2) = \left(\frac{1}{x^{\alpha' t}}\right)[q^i(x,\mu_0^2) + \bar{q}^i(x,\mu_0^2)],$$
$$g(x,t,\mu_0^2) = \left(\frac{1}{x^{\alpha'_g t}}\right) g(x,\mu_0^2), \tag{28}$$

where $q^i(x,\mu^2)$ and $\bar{q}^i(x,\mu^2)$ are quark and antiquark forward parton distributions and $g(x,\mu^2)$ is the gluon forward distribution.

The model of Eq. (28) is specified at some low normalization point. In this work, $\mu_0^2 = 1$ GeV^2. The functions $q^i(t)$ and $\bar{q}^i(t)$ at higher $\mu^2 > \mu_0^2$ are obtained by LO Dokshitzer-Gribov-Lipatov-Altarelli-Parisi (DGLAP) evolution at fixed t. While the gluon function $g(x,t,\mu^2)$ does not enter any LO expressions for DVCS observables (the handbag approximation), one still needs to specify $g(x,t,\mu_0^2)$ for the QCD evolution.

The parameters $\alpha'_{\rm val}$, α', and α'_g can be thought of as effective slopes of the corresponding Regge trajectories. For the valence quarks, we use $\alpha'_{\rm val} = 1.1(1-x)$ GeV^{-2} [36], which gives a good description of the nucleon elastic form factors. Numerically similar options for $\alpha'_{\rm val}$ were also considered in the literature [4,37–39]. All of them correspond to $\alpha'_{\rm val} \approx 0.9$–$1.0$ GeV^{-2}, which is the typical slope of all known meson and baryon Regge trajectories.

Drawing an analogy between the parameters α' and α'_g and the slope of the Pomeron trajectory $\alpha'_{\rm IP}$, one would expect that $\alpha' \approx \alpha'_g \approx \alpha'_{\rm IP} = 0.25$ GeV^{-2}. However, our analysis of the DVCS cross section in Sec. III shows that larger values should be taken. In this work, we use

$$\alpha' = 0.9\ \text{GeV}^{-2}, \qquad \alpha'_g = 0.5\ \text{GeV}^{-2}. \tag{29}$$

The inconsistency between the phenomenologically large values of α' and α'_g and the ones expected on the basis of the Regge theory was discussed in Ref. [39].

Since the D-term does not have a partonic interpretation, we cannot use the model of Eq. (28) to constrain the t dependence of the Gegenbauer moments d^i_n and, hence, the t dependence of $\tilde{Q}^i_2$. Instead, we employ the results of the lattice calculations of the t dependence of the first moments of GPDs, which were fitted to the dipole form [40], and use

$$d_n^{u,d}(t) = d_n^{u,d}(t=0)\frac{1}{(1-t/M_D^2)^2}, \tag{30}$$

where $M_D = 1.11 \pm 0.20\,\text{GeV}$ in the continuum limit [40].

Finally, the same dipole form of the t dependence was assumed for the δ-function contribution to the functions e^i and $\bar{e}^i$; see Eq. (24).

C. Predictions for the GPDs H^i and E^i

The numerical predictions for the x, ξ, and μ^2 dependence of the GPDs H^u and E^u at $t = 0$ are presented in Figs. 1–3 (see the captions).

In Fig. 1, the results of the dual parametrization are presented as solid curves. For comparison, the predictions of the DD model with the D-term added are given by dashed curves. In addition, for the $\xi = 0.1$ case, the dot-dashed curves present the calculation using the dual parametrization, when the contribution of Q_2^i is omitted. Therefore, the deviation of the dot-dashed curve from the solid curves can serve as an estimate of the theoretical uncertainty associated with the modeling of the function Q_2^i. Note that, for $\xi = 0.01$, the dot-dashed and solid curves are indistinguishable: Only the contribution of Q_0^i is important at sufficiently low ξ.

The predictions of the DD model (dashed curves) for the singlet combination of the GPDs H^i were made using the standard expressions [4,17,18]

$$\begin{aligned} H^i_{\text{DD}}(x,\xi,\mu^2) &\equiv \frac{H^i(x,\xi,\mu^2) - H^i(-x,\xi,\mu^2)}{2} \\ &= \int_{-1}^{1} d\beta \int_{-1+|\beta|}^{1-|\beta|} d\alpha[\delta(x-\beta-\alpha\xi) - \delta(-x-\beta-\alpha\xi)]h(\beta,\alpha)\frac{q^i(\beta,\mu^2)}{2} + \theta(\xi-|x|)D^i\left(\frac{x}{\xi},\mu^2\right) \\ &= \int_{0}^{1} d\beta \int_{-1+\beta}^{1-\beta} d\alpha[\delta(x-\beta-\alpha\xi) - \delta(x+\beta-\alpha\xi)]h(\beta,\alpha)\left(\frac{q^i(\beta,\mu^2)+\bar{q}^i(\beta,\mu^2)}{2}\right) \\ &\quad + \theta(\xi-|x|)D^i\left(\frac{x}{\xi},\mu^2\right), \end{aligned} \tag{31}$$

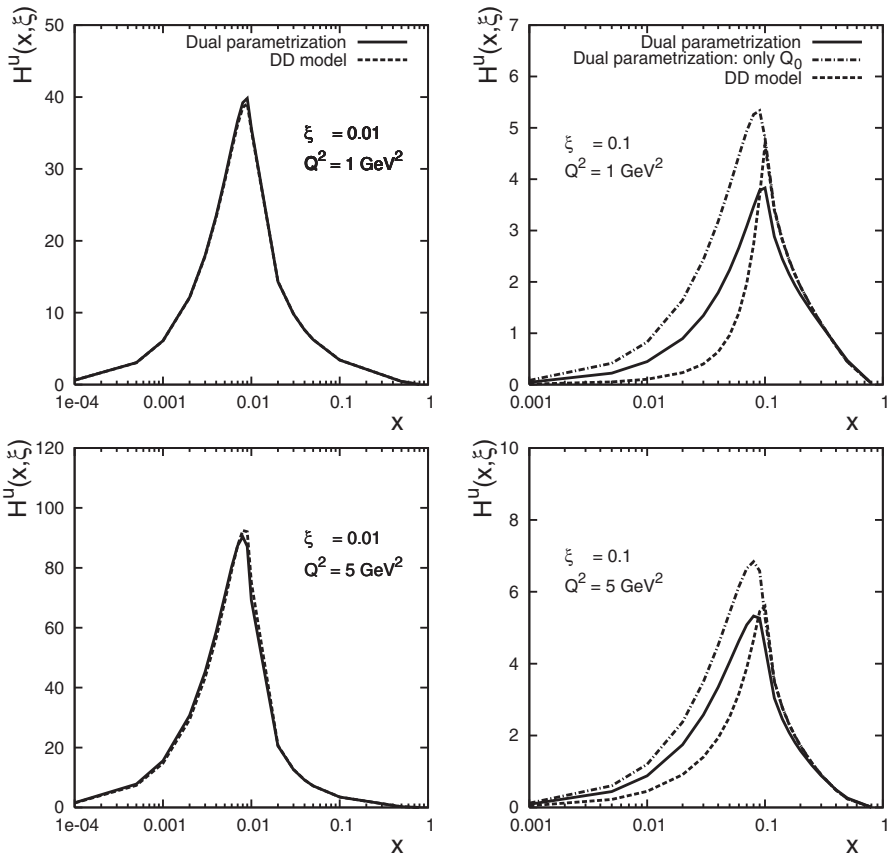

FIG. 1. The singlet GPD H^u as a function of x, ξ, and μ^2. The dual parametrization results (7) (solid curves) are compared to the predictions of the DD model (31) (dashed curves). The dot-dashed curves correspond to the dual parametrization, when only the function Q_0^i is retained.

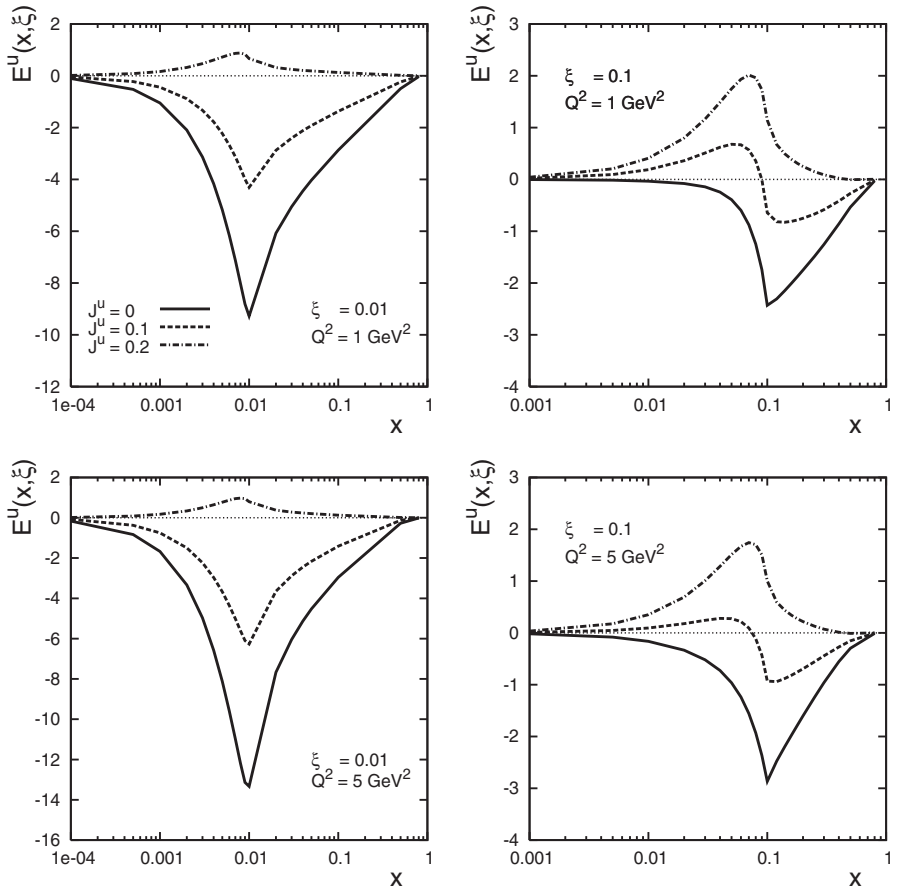

FIG. 2. The singlet GPD E^u as a function of x, ξ, and μ^2. The curves are obtained using the dual parametrization summarized in Eqs. (7), (20), (24), and (25). The solid curves correspond to $J^u = 0$; the dashed curves correspond to $J^u = 0.1$; the dot-dashed curves correspond to $J^u = 0.2$.

where

$$h(\beta, \alpha) = \frac{3}{4} \frac{(1 - |\beta|)^2 - \alpha^2}{(1 - |\beta|)^3} \tag{32}$$

and

$$D^i(z, \mu^2) = (1 - z^2) \sum_{n=1}^{5} d_n^i(\mu^2) C_n^{3/2}(z). \tag{33}$$

Note the coefficient $1/2$ in the first line of Eq. (31): It is

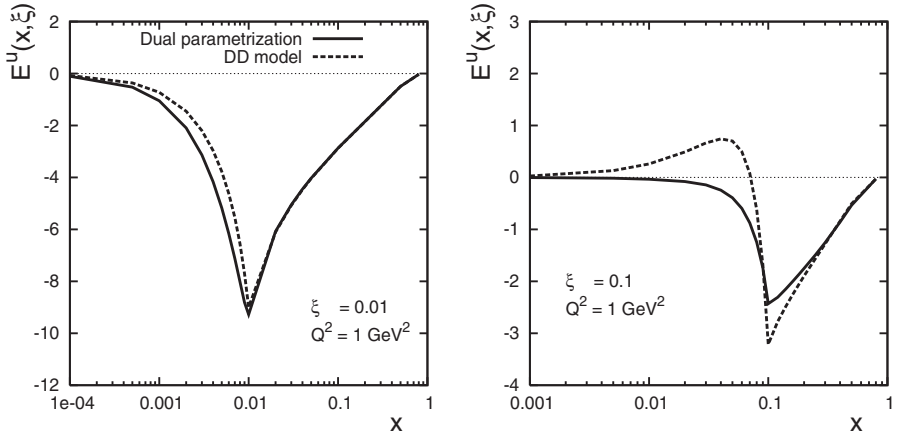

FIG. 3. The singlet GPD E^u with $J^u = 0$. The dual parametrization calculation (solid curves) is confronted with the DD model calculation (dashed curves).

required to have the correct normalization of the first moment of $H^i_{\rm DD}$.

The dual parametrization predictions for the singlet GPD E^u are summarized in Fig. 2. We would like to emphasize that the shape of the GPDs E^i is unknown. The model for the forward limit of the GPDs E^i that we used [see Eqs. (24) and (25)] was chosen rather arbitrary and, eventually, might turn out to be wrong. In this model, the shape of E^i is correlated with the fraction of the proton total orbital momentum carried by the quark, J^i. In Fig. 2, the solid curves correspond to $J^u = 0$; the dashed curves correspond to $J^u = 0.1$; the dot-dashed curves correspond to $J^u = 0.2$.

For an alternative model of GPDs E^i, we refer the reader to the calculations within the framework of the chiral quark soliton model [41].

In Fig. 3, the dual parametrization calculation of the singlet E^u with $J^u = 0$ (solid curves) is compared to the DD model calculation (dashed curves). The latter was performed using Eq. (31) after the replacement of q^i by e^i and after changing the sign in front of the D-term.

III. DVCS CROSS SECTION

The differential cross section of DVCS reads [4]

$$\frac{d\sigma}{dQ^2 dx_B dt d\phi} = \frac{1}{32(2\pi)^4}\frac{x_B y^2}{Q^4} \times \frac{e^6}{\sqrt{1+4m_N^2 x_B^2/Q^2}}|\bar{\mathcal{T}}_{\rm DVCS}|^2, \quad (34)$$

where x_B, Q^2, and $y = Q^2/(x_B s)$ ($\sqrt{s}$ is the lepton-proton invariant mass) are the usual Bjorken variables; ϕ is the angle between the plane formed by the leptons and the plane formed by the final photon and the final proton [5]; $\mathcal{T}_{\rm DVCS}$ is the full DVCS amplitude. The bar over the DVCS amplitude squared means that we have summed over the final polarization and averaged over the initial polarizations of all involved particles.

The results of high-energy DVCS measurements at HERA are usually presented in terms of the DVCS cross section on the photon level [35,42,43],

$$\sigma_{\rm DVCS}(x_B, Q^2) = \frac{1}{\Gamma}\left(\frac{x_B}{y}\right)\int dt d\phi \frac{d\sigma}{dQ^2 dx_B dt d\phi}, \quad (35)$$

where

$$\Gamma = \frac{\alpha_{\rm em}(1-y+y^2/2)}{\pi Q^2 y} \quad (36)$$

is the flux of the equivalent photons [35]. Squaring the full DVCS amplitude, averaging over initial polarization and summing over final polarizations, one obtains the following unpolarized, t-integrated DVCS cross section on the photon level:

$$\sigma_{\rm DVCS}(x_B, Q^2) = \frac{\pi\alpha_{\rm em}^2 x_B^2}{Q^4\sqrt{1+4m_N^2 x_B^2/Q^2}} \times \int_{t_{\rm min}}^{t_{\rm max}} dt |\mathcal{A}_{\rm DVCS}(\xi, t, Q^2)|^2, \quad (37)$$

where

$$|\mathcal{A}_{\rm DVCS}(\xi, t, Q^2)|^2 = |\mathcal{H}|^2(1-\xi^2) - \xi^2(\mathcal{H}^*\mathcal{E} + \mathcal{H}\mathcal{E}^*) - |\mathcal{E}|^2\left(\frac{t}{4m_N^2} + \xi^2\right) \quad (38)$$

and

$$\mathcal{H}(\xi, t, Q^2) = \sum_i e_i^2 \int_0^1 dx H^i(x, \xi, t, Q^2) \times \left(\frac{1}{x-\xi+i0} + \frac{1}{x+\xi-i0}\right),$$
$$\mathcal{E}(\xi, t, Q^2) = \sum_i e_i^2 \int_0^1 dx E^i(x, \xi, t, Q^2) \times \left(\frac{1}{x-\xi+i0} + \frac{1}{x+\xi-i0}\right). \quad (39)$$

Throughout this paper, the skewedness parameter ξ is related to the Bjorken variable x_B as $\xi = x_B/(2-x_B)$ [4]. Equations (37) and (38) for the unpolarized DVCS cross section can also be obtained from more general expressions derived in Ref. [5].

It is important to note that, in Eq. (39), we used the notation of Ref. [4], which differs from the notation of Ref. [5] by an overall minus sign. While this is immaterial for the DVCS cross section, it matters for the DVCS asymmetries.

One appealing feature of the dual parametrization of GPDs is that the convolution integrals in Eq. (39) can be readily taken and expressed in terms of the generating functions Q_n^i and R_n^i [25],

$$\mathcal{H}(\xi, t, Q^2) = -\sum_i e_i^2 \int_0^1 \frac{dx}{x}\sum_{k=0}^{\infty} x^k Q_k^i(x, t, Q^2) \times \left(\frac{1}{\sqrt{1-\frac{2x}{\xi}+x^2}} + \frac{1}{\sqrt{1+\frac{2x}{\xi}+x^2}} - 2\delta_{k0}\right),$$
$$\mathcal{E}(\xi, t, Q^2) = -\sum_i e_i^2 \int_0^1 \frac{dx}{x}\sum_{k=0}^{\infty} x^k R_k^i(x, t, Q^2) \times \left(\frac{1}{\sqrt{1-\frac{2x}{\xi}+x^2}} + \frac{1}{\sqrt{1+\frac{2x}{\xi}+x^2}} - 2\delta_{k0}\right). \quad (40)$$

The high-energy HERA data on the total DVCS cross section corresponds to very small ξ, $\xi < 0.005$, and to small t, $t < 1$ GeV^2. Therefore, the contribution of the GPD E to the DVCS cross section is negligible. Moreover, as discussed in Sec. II, at small ξ, the contribu-

tion of Q_n^i with $n \geq 2$ can be safely neglected. Therefore, our predictions for $\sigma_{\rm DVCS}$ within the framework of the dual parametrization are made keeping only the functions Q_0^i, which, up to the t dependence, are given by the forward quark distributions.

Figures 4 and 5 present our predictions for the Q^2 and W dependence of $\sigma_{\rm DVCS}$. The calculations are performed using the Regge-motivated t dependence (28) (solid curves) and the factorized exponential t dependence (26) (dashed curves). The theoretical predictions are compared to the H1 [35] and ZEUS [43] data.

Note that the ZEUS data, which were taken at $W = 89$ GeV and $Q^2 = 9.6$ GeV^2, have been rescaled to the H1 values of $W = 82$ GeV and $Q^2 = 8$ GeV^2 using the fitted W and Q^2 dependence of the DVCS cross section measured by ZEUS, $\sigma_{\rm DVCS} \propto W^{0.75}$ and $\sigma_{\rm DVCS} \propto 1/(Q^2)^{1.54}$ [43].

One can see from Fig. 4 that the absolute value and the Q^2 dependence of the total DVCS cross section are reproduced well using both the nonfactorized Regge-motivated (28) and factorized exponential (26) models of the t dependence. However, at the highest values of Q^2, the exponential model of the t dependence gives somewhat larger $\sigma_{\rm DVCS}$ because of the Q^2-dependent slope B (27), which provides a better agreement with the highest Q^2 ZEUS point.

Note that the parameters α' and α'_g of the Regge-motivated model of the t dependence [see Eq. (29)] were chosen such that the theoretical calculations reproduce well the absolute value of $\sigma_{\rm DVCS}$ in Fig. 4. Smaller values of α' and α'_g, which would be closer to $\alpha'_{\rm IP}$, would give inconsistently large values of $\sigma_{\rm DVCS}$.

From Fig. 5 one can see that the absolute value and the W dependence of $\sigma_{\rm DVCS}$ are also reproduced well. The H1 data [35] somewhat prefer the results of the calculation using the Regge-motivated t dependence. However, large experimental errors at large values of W and the discrepancy between the H1 and ZEUS data do not allow one to draw a more quantitative conclusion.

In addition to the t-integrated DVCS cross section, for the first time, the H1 reported the differential DVCS cross section [35]. The dual parametrization predictions for $d\sigma_{\rm DVCS}/dt$ as a function of t are compared to the H1 data in Fig. 6. The theoretical predictions are made using Eq. (37) without the integration over t,

$$\frac{d\sigma_{\rm DVCS}(x_B, t, Q^2)}{dt} = \frac{\pi \alpha_{\rm em}^2 x_B^2}{Q^4 \sqrt{1 + 4m_N^2 x_B^2/Q^2}} |\mathcal{A}_{\rm DVCS}(\xi, t, Q^2)|^2. \tag{41}$$

As one can see from Fig. 6, for $|t| < 0.5$ GeV^2 both models of the t dependence give rather similar predictions and describe the data well. However, for $|t| > 0.5$ GeV^2, the exponential model corresponds to a steeper decrease of $d\sigma_{\rm DVCS}/dt$ with increasing $|t|$ and allows us to describe the highest $|t| = 0.8$ GeV^2 data point very well. The experimental errors on $d\sigma_{\rm DVCS}/dt$ are small enough to conclude that the Regge-motivated model of the t dependence of GPDs (29) seems to be disfavored by the large-$|t|$ H1 data [35].

It is important to appreciate that, within the framework of the dual parametrization of GPDs, the HERA data on the DVCS cross section were described so well without any free parameters: We used only the forward parton distri-

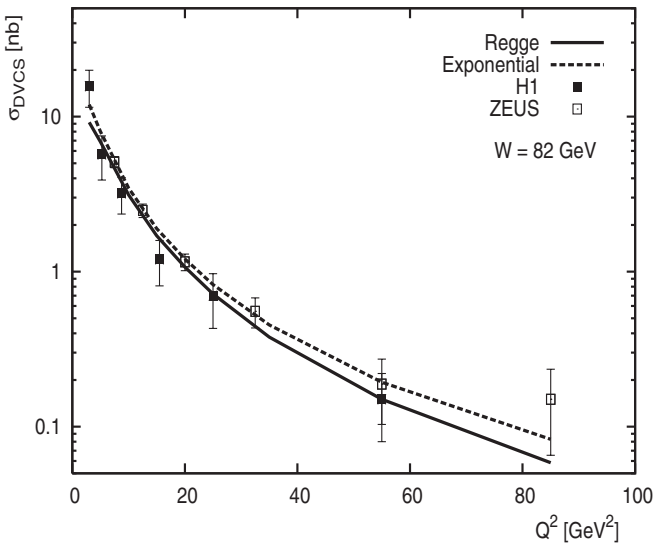

FIG. 4. The total DVCS cross section $\sigma_{\rm DVCS}$ as a function of Q^2 at fixed W. The dual parametrization predictions are given by the solid (Regge model for the t dependence) and dashed (factorized exponential t dependence) curves. The experimental points are H1 [35] and ZEUS [43]. The statistical and systematic experimental errors are added in quadrature.

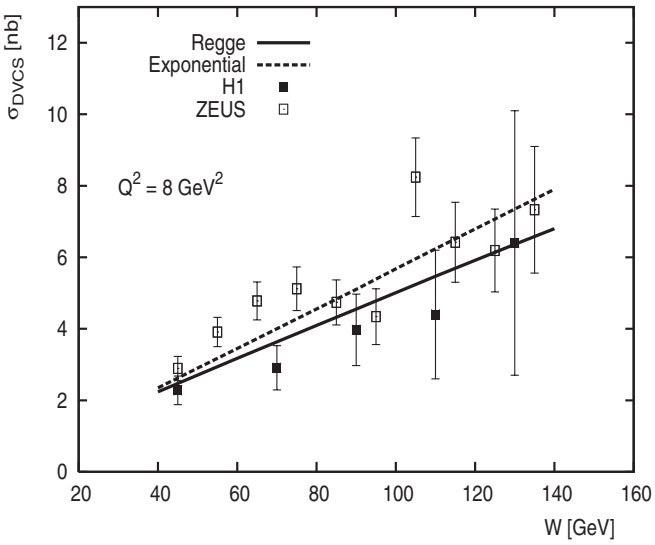

FIG. 5. The total DVCS cross section $\sigma_{\rm DVCS}$ as a function of W at fixed Q^2. The captions are the same as in Fig. 4.

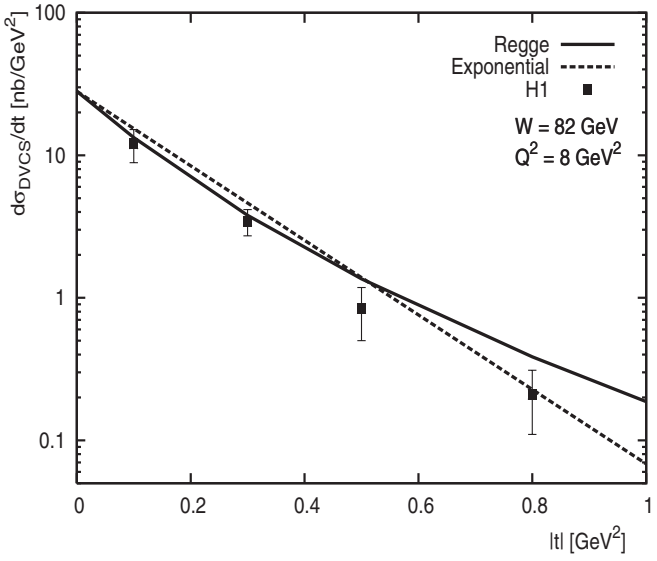

FIG. 6. The differential DVCS cross section as a function of $|t|$. The dual parametrization predictions (solid and dashed curves; see details in the caption to Fig. 4) are compared to the H1 data [35].

butions for the input. To be more precise, the parameters α' and α'_g were adjusted to reproduce only the normalization of the DVCS cross section: The Q^2, W, and t-dependencies of the cross section were then predicted without any further adjustments. The calculation using the factorized exponential t dependence contained no free adjustable parameters since the slope $B(\mu)$ (27) has been experimentally measured [35] and, hence, it could not be varied.

The DVCS cross section can also be described using other models of GPDs. Within the framework of the double distribution model, the H1 and ZEUS data on $\sigma_{\rm DVCS}$ were successfully described with the asymptotic ansatz for $h(\beta, \alpha)$ in Eq. (31), which corresponds to the ξ-independent input, $H^i_{\rm DD}(x, \xi, \mu_0^2) = (q^i(x, \mu_0^2) + \bar{q}^i(x, \mu_0^2))/2$ [5,21]. The observation that the DVCS cross section at high energies (small x_B) and at high Q^2 can be described by the GPDs, whose shape at the low input scale μ_0^2 is ξ-independent, can be qualitatively explained as follows. Under QCD evolution, a GPD at a given small x and large μ^2 is obtained using the GPD at the low input scale μ_0^2, which is probed for $x_0 \gg x$. Therefore, the small external parameter ξ can be neglected in the input GPDs [44].

Other theoretical approaches, which enable one to successfully describe the HERA data on $\sigma_{\rm DVCS}$, include the dipole formalism [45,46] and the formalism based on the conformal moments of the GPDs [47].

IV. DVCS ASYMMETRIES

Complete expressions for various DVCS asymmetries are well known [5]. In this work, we consider the beam-spin $A_{\rm LU}$, beam-charge A_C, and transversely polarized target $A_{\rm UT}$ asymmetries. The first two asymmetries are predominantly sensitive to the GPD H, while the $A_{\rm UT}$ asymmetry is sensitive to both GPDs H and E. Since most of the data on these DVCS asymmetries have come from the HERMES Collaboration at DESY [48–55], we will predominantly make numerical predictions for the above asymmetries using the dual parametrization of GPDs H and E in the HERMES kinematics. In addition, predictions for the Jefferson Lab kinematics will also be presented.

A. Beam-spin asymmetry

Using results of Ref. [5], one obtains the following approximate expression for the $\sin\phi$ moment of the beam-spin asymmetry:

$$A_{\rm LU}^{\sin\phi} \approx +\left(\frac{x_B}{y}\right) 8Ky(2-y)(1+\epsilon^2)^2 \times \frac{[F_1(t)\,{\rm Im}\mathcal{H}(\xi,t,Q^2) + \frac{|t|}{4m_N^2}F_2(t)\,{\rm Im}\mathcal{E}(\xi,t,Q^2)]}{c^{\rm BH}_{0,\rm unp}}, \quad (42)$$

where $\epsilon = x_B m_N/Q$; the kinematic suppression factor K and the leading harmonic of the Bethe-Heitler amplitude squared $c^{\rm BH}_{0,\rm unp}$ are given in [5]; F_1 and F_2 are the Dirac and Pauli proton form factors (see e.g. [5]); $\mathcal{H}$ and $\mathcal{E}$ are defined by Eq. (40). Equation (42) is approximate because we have neglected subleading harmonics (proportional to $c^{\rm BH}_{1,\rm unp}$ and $c^{\rm BH}_{2,\rm unp}$) in the expansion of the Bethe-Heitler amplitude squared and the DVCS amplitude squared in the denominator of Eq. (42).

Note that we have introduced an additional minus sign in order to take into account the sign difference between our notation for $\mathcal{H}$ and the notation of Ref. [5]. Therefore, in Eq. (42), the plus sign corresponds to the positively charged lepton beam. Since in our notation ${\rm Im}\mathcal{H} < 0$ in the bulk of the considered kinematics, $A_{\rm LU}^{\sin\phi}$ in the HERMES kinematics is negative.

One should point out that we use the reference frame of Ref. [5], which differs from the frame used by the HERMES Collaboration by the direction of the z axis (the Trento sign conventions [56]). This means that $\phi_{\rm HERMES} = \pi - \phi$ [5,57]. Obviously, for the $\sin\phi$ moment of the beam-spin asymmetry, this difference in the notations is irrelevant.

Using the dual parametrization of GPD discussed in Sec. II and substituting it in Eq. (42), we obtain the following range of predictions at the average kinematic point of the HERMES measurement, $\langle x_B\rangle = 0.11$, $\langle Q^2\rangle = 2.6$ GeV^2, and $\langle t\rangle = -0.27$ GeV^2 [48],

$$A_{\rm LU}^{\sin\phi} = -0.22\ldots-0.24, \quad \text{exponential } t \text{ dependence},$$
$$A_{\rm LU}^{\sin\phi} = -0.27\ldots-0.29, \quad \text{Regge } t \text{ dependence}. \quad (43)$$

The smaller absolute values of $A_{\mathrm{LU}}^{\sin\phi}$ correspond to the calculation with $J_u = J_d = 0$; the larger absolute values of $A_{\mathrm{LU}}^{\sin\phi}$ correspond to the calculation with $J_u = 0.3$ and $J_d = 0$ (the variation of J_d has no noticeable effect). As expected, the small range of predictions (for a given model of the t dependence) indicates small sensitivity of $A_{\mathrm{LU}}^{\sin\phi}$ to the GPD E.

Our theoretical calculations compare very well to the HERMES measurement [48]

$$A_{\mathrm{LU}}^{\sin\phi} = -0.23 \pm 0.04 \pm 0.03. \tag{44}$$

In addition to the average HERMES kinematics, we studied the dependence of $A_{\mathrm{LU}}^{\sin\phi}$ on t, x_B, and Q^2 bin by bin [51,57]. Figure 7 summarizes our predictions, which are made using $J_u = J_d = 0$.

As can be seen from Fig. 7, only $A_{\mathrm{LU}}^{\sin\phi}$ as a function of $|t|$ can be helpful in distinguishing between the exponential and Regge models of the t dependence, provided the experimental uncertainties are sufficiently small.

We also make predictions for the beam-spin asymmetry in the CLAS kinematics. For the 2001 average kinematic point of the CLAS kinematics [58], $E = 4.25$ GeV, $\langle Q^2 \rangle = 1.25$ GeV^2, $\langle x_B \rangle = 0.19$, and $\langle t \rangle = -0.19$ GeV^2, our predictions compare very well to the experimental value,

$$\begin{aligned} A_{\mathrm{LU}}^{\sin\phi} &= 0.15 \ldots 0.17, && \text{exponential } t \text{ dependence,} \\ A_{\mathrm{LU}}^{\sin\phi} &= 0.18 \ldots 0.20, && \text{Regge } t \text{ dependence,} \\ A_{\mathrm{LU}}^{\sin\phi} &= 0.202 \pm 0.028, && \text{CLAS [58].} \end{aligned} \tag{45}$$

The lower values of the theoretical predictions correspond to $J_u = J_d = 0$; the larger values correspond to $J_u = 0.3$ and $J_d = 0$. Note the sign change in $A_{\mathrm{LU}}^{\sin\phi}$ when going from the positron beam (HERMES) to the electron beam (CLAS).

Recently, CLAS performed dedicated measurements of DVCS and, in particular, of the beam-spin asymmetry with higher energies of the lepton beam and with much wider kinematic coverage in Q^2, x_B, and t. Figure 8 presents our predictions for the t dependence of $A_{\mathrm{LU}}^{\sin\phi}$ at $E = 5.7$ GeV, $Q^2 = 1.5$ GeV^2, and $x_B = 0.25$.

It is important to point out that, by construction, the minimal model of the dual parametrization of GPDs is designed for small values of x_B, $x_B \leq 0.2$. The increase of x_B from $x_B \approx 0.2$ (HERMES) to $x_B \approx 0.3$ (current

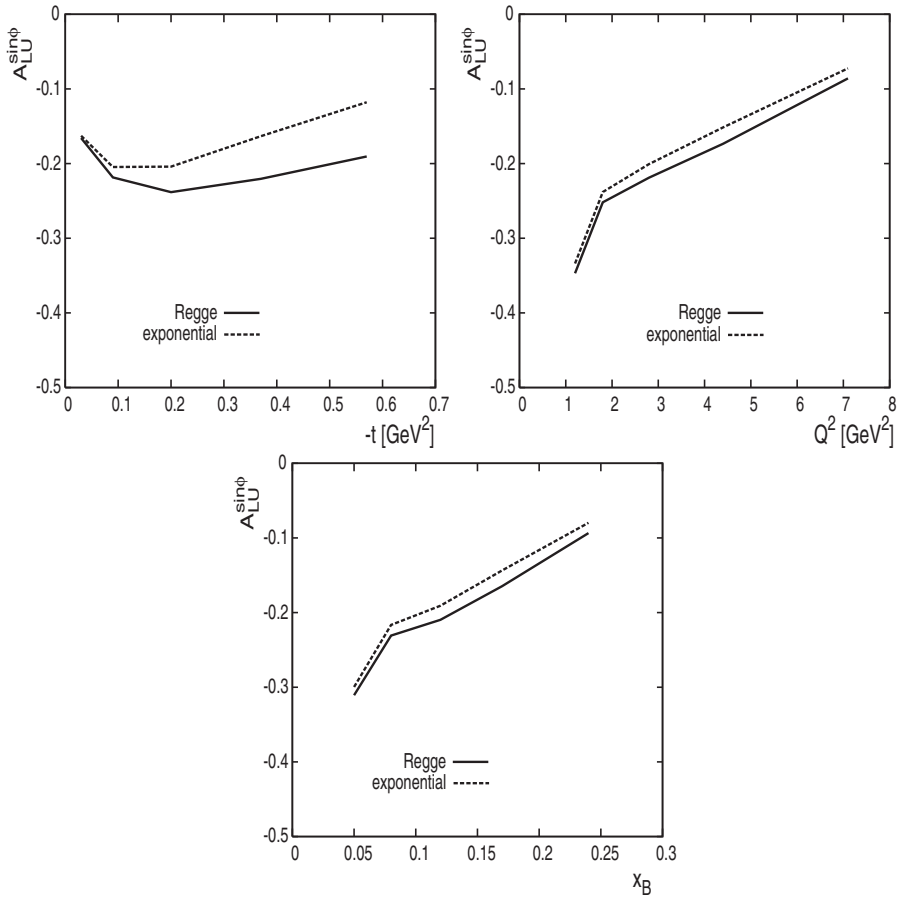

FIG. 7. $A_{\mathrm{LU}}^{\sin\phi}$ as a function of t, x_B, and Q^2. The dual parametrization predictions with two models of the t dependence in the HERMES kinematics [51] are given by the solid and dotted curves.

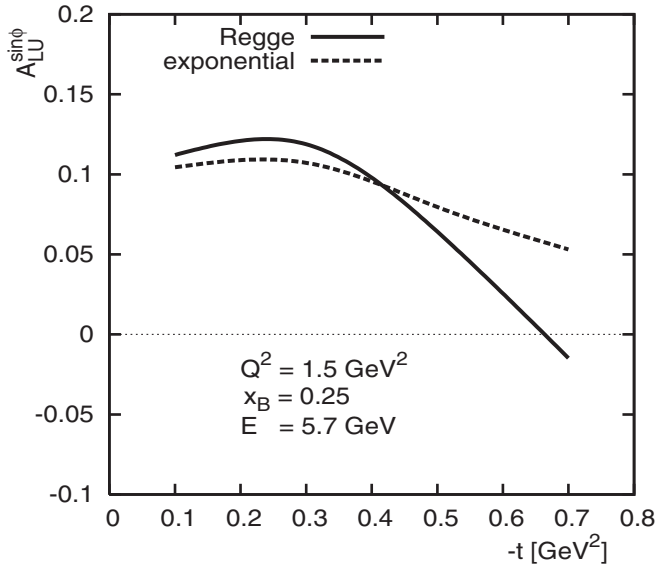

FIG. 8. $A_{\rm LU}^{\sin\phi}$ as a function of t in the CLAS kinematics. The two curves represent calculations with two models of the t dependence (see the text).

CLAS) leads to the increasing role of the generating functions Q_2^i and R_2^i (the latter plays a role at large $|t|$, $|t| > 0.5$ GeV^2), which results in a significant model dependence of our results. Therefore, our predictions in Fig. 8 should be taken as semiquantitative. Strictly speaking, in order to make quantitative predictions for the current CLAS kinematics, one has to extend the minimal model by including higher generating functions Q_k^i and R_k^i with $k \geq 4$.

B. Beam-charge asymmetry

Next we turn to the beam-charge asymmetry, A_C. Using the results of Ref. [5], the approximate expression for A_C reads [we have neglected the same terms in the denominator as in Eq. (42)]

$$A_C(\phi) \approx \left(\frac{x_B}{y}\right)(1+\epsilon^2)^2 \frac{c_{0,\rm unp}^I + c_{1,\rm unp}^I \cos\phi}{c_{0,\rm unp}^{\rm BH}}, \qquad (46)$$

where $c_{0,\rm unp}^I$ and $c_{1,\rm unp}^I$ are given in Ref. [5]. While $c_{0,\rm unp}^I$ is smaller than $c_{1,\rm unp}^I$, it is not negligibly small. In this work, we shall concentrate on the larger contribution to A_C proportional to $c_{1,\rm unp}^I$, which can be singled out by considering the $\cos\phi$ moment of A_C,

$$A_C^{\cos\phi} \approx -\left(\frac{x_B}{y}\right) 8K(2-2y+y^2)(1+\epsilon^2)^2 \times \frac{[F_1(t)\,{\rm Re}\mathcal{H}(\xi,t,Q^2) + \frac{|t|}{4m_N^2}F_2(t)\,{\rm Re}\mathcal{E}(\xi,t,Q^2)]}{c_{0,\rm unp}^{\rm BH}}. \qquad (47)$$

As discussed above, $\phi_{\rm HERMES} = \pi - \phi$. Therefore, $A_C^{\cos\phi_{\rm HERMES}} = -A_C^{\cos\phi}$. Since in the considered kinematics ${\rm Re}\mathcal{H} > 0$, we obtain $A_C^{\cos\phi_{\rm HERMES}} > 0$. Until the end of this subsection, we shall imply $\phi_{\rm HERMES}$, but we will use ϕ for brevity.

The range of predictions for $A_C^{\cos\phi}$ using the dual parametrization of GPDs can be compared to the HERMES measurements. For the 2002 HERMES average kinematic point, $\langle x_B\rangle = 0.12$, $\langle Q^2\rangle = 2.8$ GeV^2, and $\langle t\rangle = -0.27$ GeV^2 [50], we obtain

$$A_C^{\cos\phi} = 0.01\ldots0.03, \quad \text{exponential } t \text{ dependence},$$
$$A_C^{\cos\phi} = 0.19\ldots0.23, \quad \text{Regge } t \text{ dependence},$$
$$A_C^{\cos\phi} = 0.11 \pm 0.04 \pm 0.03, \quad \text{HERMES [50]}. \qquad (48)$$

The lower values of $A_C^{\cos\phi}$ correspond to the calculation with $J_u = J_d = 0$; the larger values correspond to $J_u = 0.3$ and $J_d = 0$.

For the very recent 2006 HERMES average kinematic point, $\langle x_B\rangle = 0.10$, $\langle Q^2\rangle = 2.5$ GeV^2, and $\langle t\rangle = -0.12$ GeV^2 [55], we obtain

$$A_C^{\cos\phi} = 0.013\ldots0.022, \quad \text{exponential } t \text{ dependence},$$
$$A_C^{\cos\phi} = 0.080\ldots0.092, \quad \text{Regge } t \text{ dependence},$$
$$A_C^{\cos\phi} = 0.063 \pm 0.029 \pm 0.026, \quad \text{HERMES [55]}. \qquad (49)$$

The following two features of Eqs. (48) and (49) deserve further discussion. First, the exponential model of the t dependence predicts the values of $A_C^{\cos\phi}$, which are much smaller than those calculated with the Regge model of the t dependence. The reasons for this are the nontrivial t dependence of the real part of $\mathcal{H}$ (more precisely, the nontrivial cancellation between two contributions to the real part of $\mathcal{H}$) and the large values of $|t|$ involved.

Second, predictions with the exponential model of the t dependence are much more sensitive to the fraction of proton spin carried by the quarks, J^i.

In addition to the average kinematic point, the recent HERMES analysis [55] presented $A_C^{\cos\phi}$ as a function of t.

Figure 9 presents the comparison of our theoretical predictions to the data. It can be seen from Fig. 9 that the Regge model describes the data points well for $|t| < 0.2$ GeV^2 and underestimates the asymmetry for the larger $|t| \approx 0.4$ GeV^2. The exponential model of the t dependence dramatically fails to describe the rise of $A_C^{\cos\phi}$ with increasing $|t|$. Therefore, on the basis of the comparison of our theoretical predictions to the t dependence of the $\cos\phi$ moment of the beam-charge asymmetry, we conclude that the nonfactorized Regge model of the t dependence of GPDs is preferred over the factorized exponential model.

In addition to the t dependence of $A_C^{\cos\phi}$, we make predictions for the Q^2 and x_B dependence of $A_C^{\cos\phi}$ in the

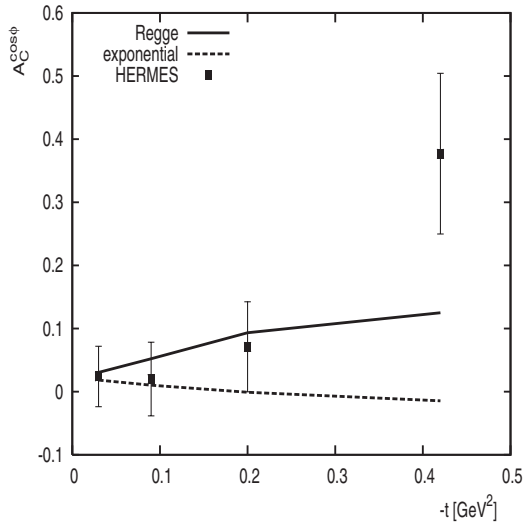

FIG. 9. $A_C^{\cos\phi}$ as a function of t. The dual parametrization predictions with two models of the t dependence are compared to the HERMES data [55].

HERMES kinematics [51,57] in Fig. 10. Our theoretical predictions are made using $J_u = J_d = 0$.

C. Transversely polarized target asymmetry

The DVCS asymmetry with the unpolarized beam and the transversely polarized target, $A_{\rm UT}$, is sensitive to all four GPDs of the nucleon [5]. Since we are concerned with the GPDs H and E, we shall consider the $\sin\varphi\cos\phi$ moment of $A_{\rm UT}$, where the angle φ is the angle between the vector of the target polarization and the hadron scattering plane in the notation of Ref. [5]. The main interest in considering this DVCS observable is that it is sensitive to the GPD E and, hence, to the fraction of the proton total angular momentum carried by quarks, J^i.

According to the Trento sign convention [56], it is recommended to use different angles, which are used e.g. in the HERMES analysis: $\phi_{\rm HERMES} = \pi - \phi$ and $\phi_{\rm S,HERMES} - \phi_{\rm HERMES} = \pi + \varphi$ [57]. Obviously, $A_{\rm UT}^{\sin\varphi\cos\phi} = A_{\rm UT}^{\sin(\phi_{\rm S,HERMES}-\phi_{\rm HERMES})\cos\phi_{\rm HERMES}}$.

Using the results [5], the approximate expression for $A_{\rm UT}^{\sin\varphi\cos\phi}$ reads

$$A_{\rm UT}^{\sin\varphi\cos\phi} \approx \left(\frac{x_B}{y}\right)(1+\epsilon^2)^2 \frac{1}{c_{0,\rm unp}^{\rm BH}} \frac{8m_N\sqrt{1-y}}{Q}(2-2y+y^2) \times \left[\frac{1}{2-x_B}\left(x_B^2 F_1(t) - (1-x_B)\frac{t}{m_N^2}F_2(t)\right) \times {\rm Im}\mathcal{H}(\xi,t,Q^2) + \left(\frac{x_B^2}{2-x_B}F_1(t) + \frac{t}{4m_N^2}\left((2-x_B)F_1(t) + \frac{x_B^2}{2-x_B}F_2(t)\right)\right){\rm Im}\mathcal{E}(\xi,t,Q^2)\right]. \quad (50)$$

Note that, similarly to the above considered $A_{\rm LU}^{\sin\phi}$ and $A_C^{\cos\phi}$, we have introduced an additional minus sign to compensate for the sign difference between our definition of $\mathcal{H}$ and $\mathcal{E}$ and the notation of Ref. [5].

The theoretical predictions for the t, Q^2, and x_B dependence of $A_{\rm UT}^{\sin\varphi\cos\phi}$ using the dual parametrization of GPDs and Eq. (50) are compared to the preliminary HERMES data [53] in Fig. 11. Note that the error bars shown correspond to the statistical and systematic uncertainties added in quadrature and that the systematic uncertainty does not include the effect of the HERMES acceptance.

The plots for the t and Q^2 dependence appear to be most informative. As can be seen from the upper and middle panels of Fig. 11, our theoretical calculations reproduce the data fairly well, except for one point. Judging by the central experimental values, one concludes that the data seems to prefer the scenario with $J_u = J_d = 0$.

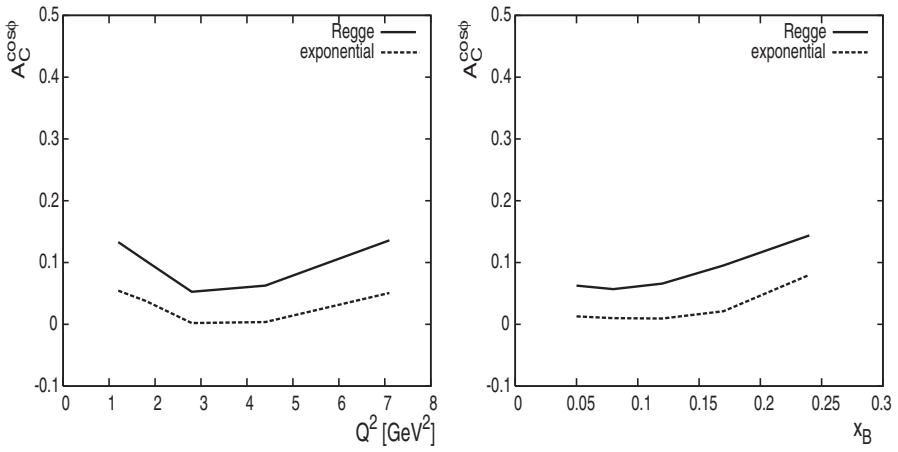

FIG. 10. $A_C^{\cos\phi}$ as a function of Q^2 and x_B. The dual parametrization predictions with two models of the t dependence in the HERMES kinematics [51] are given by the solid and dotted curves.

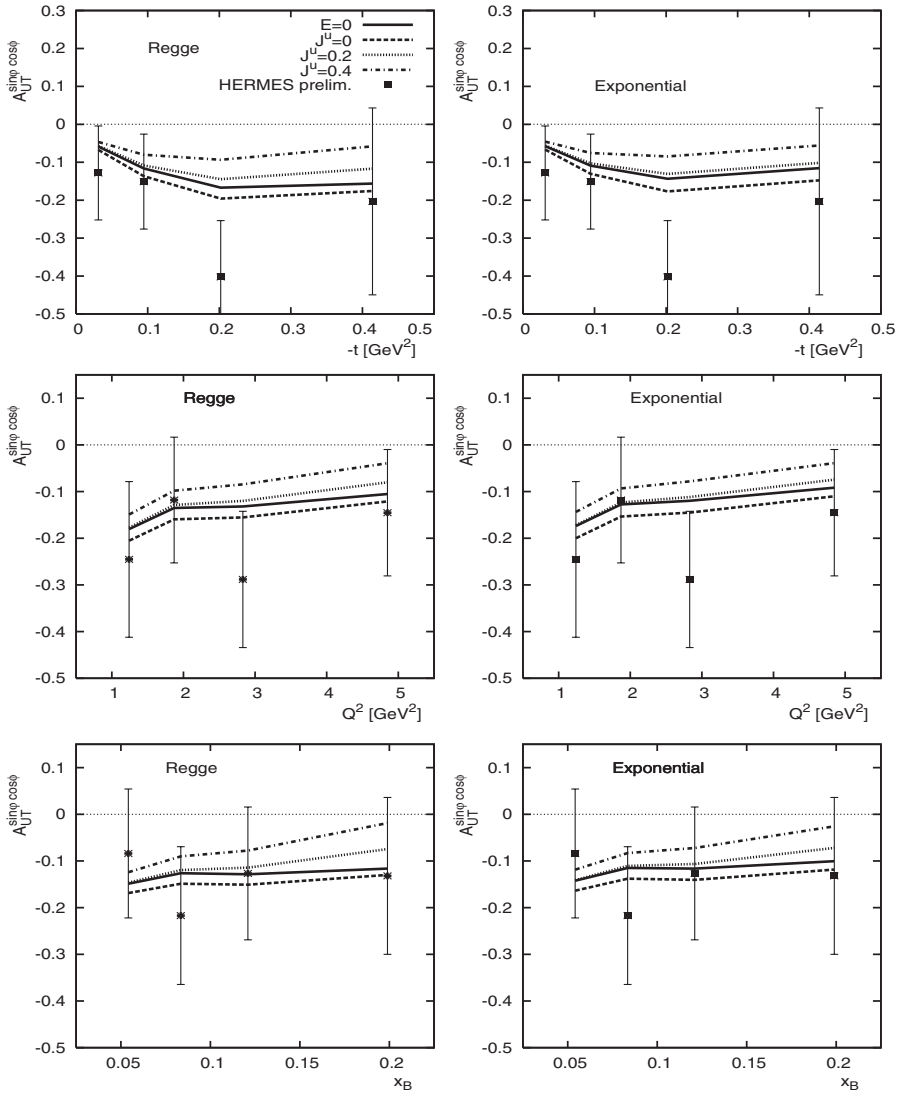

FIG. 11. $A_{\rm UT}^{\sin\varphi\cos\phi}$ as a function of t, x_B, and Q^2. The dual parametrization predictions with two models of the t dependence are compared to the HERMES preliminary data [53]. The error bars correspond to the statistical and systematic uncertainties added in quadrature. The systematic uncertainty does not include the effect of the HERMES acceptance.

Also, both models of the t dependence give rather close results. Therefore, in view of large experimental uncertainties, it is impossible to differentiate between the Regge and exponential models of the t dependence of the GPDs using the current preliminary HERMES data on $A_{\rm UT}^{\sin\varphi\cos\phi}$ [53].

In addition, we compare our predictions for $A_{\rm UT}^{\sin\varphi\cos\phi}$ to the HERMES measurement at the average kinematic point, $\langle x_B\rangle = 0.095$, $\langle Q^2\rangle = 2.5$ GeV^2, and $\langle -t\rangle = 0.12$ GeV^2 [54],

$$\begin{aligned} A_{\rm UT}^{\sin\varphi\cos\phi} &= -0.14\ldots-0.10, \quad \text{exponential } t \text{ dependence},\\ A_{\rm UT}^{\sin\varphi\cos\phi} &= -0.15\ldots-0.10, \quad \text{Regge } t \text{ dependence},\\ A_C^{\cos\phi} &= -0.149\pm0.058\pm0.033,\\ &\quad \text{prelim. HERMES [54]}. \end{aligned} \tag{51}$$

The lower absolute values of $A_{\rm UT}^{\sin\varphi\cos\phi}$ correspond to the calculation with $J_u = J_d = 0$; the larger values correspond to $J_u = 0.3$ and $J_d = 0$. As can be seen from Eq. (51), the agreement between our predictions and the experimental value is very good. The central experimental value prefers $J_u = J_d = 0$.

Predictions for $A_{\rm UT}^{\sin\varphi\cos\phi}$ were also made within the framework of the double distribution model of GPDs [57]. The comparison of the theoretical predictions [57] to the HERMES data [53] does not allow one to make a definite conclusion about the fraction of the proton total angular momentum carried by the u-quark: The data on the t dependence somewhat prefer $J_u = 0$ and $J_u = 0.2$, while the data on x_B and Q^2 dependence prefer $J_u = 0.2$ and $J_u = 0.4$.

In conclusion of this short discussion of the fraction of the total angular momentum of the proton carried by

quarks, we would like to mention the lattice results of the QCDSF Collaboration: $J^u = 0.37 \pm 0.06$ and $J^d = -0.04 \pm 0.04$ [40]. Our analysis presented in this section indicates that the value of J^u should be significantly smaller.

V. CONCLUSIONS AND DISCUSSION

In this work, we considered the new LO dual parametrization of GPDs introduced by Polyakov and Shuvaev [25]. The advantages of the dual parametrization include simple (forward) QCD evolution of resulting GPDs and a simple expression for the LO DVCS amplitude. We extended the work by Guzey and Polyakov [24] and formulated the minimal model of the dual parametrization of GPDs H^i and E^i, which enables one to relate the GPDs to the fairly well-known quantities. In particular, apart from the t dependence, the GPDs H^i can be formulated in terms of the forward quark distributions q^i and Gegenbauer moments of the D-term. The GPDs E^i can be formulated in terms of the unknown forward limit of the GPDs E^i and, again, the Gegenbauer moments of the D-term. The price to pay for the simplicity of our dual model is that the model is designed for not too large x_B, $x_B \leq 0.2$. Within the considered model, the t dependence of GPDs has to be modeled separately. We considered two different models of the t dependence: the factorized exponential model and the nonfactorized Regge-motivated model.

We compared predictions of our model to all available data on the DVCS cross section and asymmetries. The Q^2, W, and t dependence of the DVCS cross section at high energies (small ξ) measured by the H1 and ZEUS collaborations was successfully described by both models of the t dependence. It should be stressed that our predictions for σ_{DVCS} are virtually model independent: Only the normalization of the cross section at one kinematic point was fitted by appropriately choosing the effective slope parameters in the Regge-motivated model of the t dependence.

Turning to the beam-spin DVCS asymmetry, A_{LU}, we successfully described both HERMES and CLAS data on $A_{\mathrm{LU}}^{\sin\phi}$ at their respective average kinematic points. We also made predictions for the t, Q^2, and x_B dependence of $A_{\mathrm{LU}}^{\sin\phi}$ in the HERMES kinematics bin by bin and for the t dependence of $A_{\mathrm{LU}}^{\sin\phi}$ in the CLAS kinematics with $E = 5.7$ GeV. We observed that only the t dependence of $A_{\mathrm{LU}}^{\sin\phi}$ has a chance to distinguish between the two considered models of the t dependence.

We found that, within our framework, the beam-charge asymmetry A_C is the only considered observable which distinguishes between the Regge-motivated and exponential models of the t dependence of GPDs. While the Regge-motivated model provides a reasonable description of $A_C^{\cos\phi}$ in the average HERMES kinematics and of the t dependence of $A_C^{\cos\phi}$ measured at HERMES, the exponential model of the t dependence fails dramatically.

We also compared our predictions to the HERMES measurement of the DVCS asymmetry measured with the unpolarized beam and the transversely polarized target, A_{UT}. We obtained a fairly good description of the preliminary HERMES data on t, Q^2, and x_B dependence of $A_{\mathrm{UT}}^{\sin\varphi\cos\phi}$ using both models of the t dependence. While the experimental uncertainties are large, the data still seems to indicate that, within our model, $J_u = J_d \approx 0$, i.e. that the u and d quarks carry only a small fraction of the proton total angular momentum.

All comparisons to the experimental values presented in this work were done taking the minimal version of the dual parametrization of GPDs at its face value. We did not take into account such potentially important effects as next-to-leading-order corrections and higher twist effects. Their role in the context of the dual parametrization of GPDs is a subject of a separate analysis.

In conclusion, the dual parametrization of GPDs presents a new model of GPDs, which, with a small number of model-dependent inputs, allows for a uniform description of all available data on the DVCS cross section and asymmetries.

ACKNOWLEDGMENTS

The authors would like to thank Z. Ye and D. Hasch for providing us with the preliminary HERMES data on $A_{\mathrm{UT}}^{\sin\varphi\cos\phi}$. V. G. would also like to thank D. Müller for useful comments.

[1] D. Mueller, D. Robaschik, B. Geyer, F. M. Dittes, and J. Horejsi, Fortschr. Phys. **42**, 101 (1994).
[2] X. D. Ji, J. Phys. G **24**, 1181 (1998).
[3] A. V. Radyushkin, hep-ph/0101225.
[4] K. Goeke, M. V. Polyakov, and M. Vanderhaeghen, Prog. Part. Nucl. Phys. **47**, 401 (2001).
[5] A. V. Belitsky, D. Muller, and A. Kirchner, Nucl. Phys. **B629**, 323 (2002).
[6] M. Diehl, Phys. Rep. **388**, 41 (2003).
[7] A. V. Belitsky and A. V. Radyushkin, Phys. Rep. **418**, 1 (2005).
[8] J. C. Collins and A. Freund, Phys. Rev. D **59**, 074009 (1999).
[9] J. C. Collins, L. Frankfurt, and M. Strikman, Phys. Rev. D **56**, 2982 (1997).
[10] X. D. Ji, W. Melnitchouk, and X. Song, Phys. Rev. D **56**,

5511 (1997).
[11] V. Y. Petrov, P. V. Pobylitsa, M. V. Polyakov, I. Bornig, K. Goeke, and C. Weiss, Phys. Rev. D **57**, 4325 (1998).
[12] B. C. Tiburzi and G. A. Miller, Phys. Rev. C **64**, 065204 (2001); Phys. Rev. D **65**, 074009 (2002).
[13] B. C. Tiburzi and G. A. Miller, Phys. Rev. D **67**, 113004 (2003).
[14] S. Scopetta and V. Vento, Phys. Rev. D **69**, 094004 (2004); **71**, 014014 (2005).
[15] B. C. Tiburzi, W. Detmold, and G. A. Miller, Phys. Rev. D **70**, 093008 (2004).
[16] H. Mineo, S. N. Yang, C. Y. Cheung, and W. Bentz, Nucl. Phys. B, Proc. Suppl. **141**, 281 (2005).
[17] A. V. Radyushkin, Phys. Rev. D **59**, 014030 (1999); Phys. Lett. B **449**, 81 (1999).
[18] I. V. Musatov and A. V. Radyushkin, Phys. Rev. D **61**, 074027 (2000).
[19] P. V. Pobylitsa, Phys. Rev. D **67**, 094012 (2003).
[20] M. V. Polyakov and C. Weiss, Phys. Rev. D **60**, 114017 (1999).
[21] A. Freund and M. McDermott, Eur. Phys. J. C **23**, 651 (2002).
[22] A. Freund, Eur. Phys. J. C **31**, 203 (2003).
[23] M. V. Polyakov, Phys. Lett. B **555**, 57 (2003).
[24] V. Guzey and M. V. Polyakov, Eur. Phys. J. C **46**, 151 (2006).
[25] M. V. Polyakov and A. G. Shuvaev, hep-ph/0207153.
[26] M. V. Polyakov, Nucl. Phys. **B555**, 231 (1999).
[27] V. De Alfaro, S. Fubini, G. Furlan, and C. Rossetti, *Current in Hadron Physics* (North-Holland Publishing Company, Amsterdam, 1973), p. 571.
[28] A. V. Belitsky, B. Geyer, D. Mueller, and A. Schafer, Phys. Lett. B **421**, 312 (1998).
[29] G. P. Lepage and S. J. Brodsky, Phys. Lett. **87B**, 359 (1979).
[30] A. V. Efremov and A. V. Radyushkin, Phys. Lett. **94B**, 245 (1980).
[31] R. Mainz, Diploma thesis, Ruhr-Universität Bochum, 2002.
[32] N. Kivel, M. V. Polyakov, and M. Vanderhaeghen, Phys. Rev. D **63**, 114014 (2001).
[33] H. L. Lai *et al.* (CTEQ Collaboration), Eur. Phys. J. C **12**, 375 (2000).
[34] A. Freund, M. McDermott, and M. Strikman, Phys. Rev. D **67**, 036001 (2003).
[35] A. Aktas *et al.* (H1 Collaboration), Eur. Phys. J. C **44**, 1 (2005).
[36] M. Guidal, M. V. Polyakov, A. V. Radyushkin, and M. Vanderhaeghen, Phys. Rev. D **72**, 054013 (2005).
[37] M. Vanderhaeghen, Nucl. Phys. **A711**, 109 (2002).
[38] M. Diehl, T. Feldmann, R. Jakob, and P. Kroll, Eur. Phys. J. C **39**, 1 (2005).
[39] M. Diehl, hep-ph/0510221.
[40] M. Gockeler, R. Horsley, D. Pleiter, P. E. L. Rakow, A. Schafer, G. Schierholz, and W. Schroers (QCDSF Collaboration), Phys. Rev. Lett. **92**, 042002 (2004).
[41] J. Ossmann, M. V. Polyakov, P. Schweitzer, D. Urbano, and K. Goeke, Phys. Rev. D **71**, 034011 (2005).
[42] C. Adloff *et al.* (H1 Collaboration), Phys. Lett. B **517**, 47 (2001).
[43] S. Chekanov *et al.* (ZEUS Collaboration), Phys. Lett. B **573**, 46 (2003).
[44] L. Frankfurt, A. Freund, V. Guzey, and M. Strikman, Phys. Lett. B **418**, 345 (1998); **429**, 414(E) (1998).
[45] L. Favart and M. V. T. Machado, Eur. Phys. J. C **29**, 365 (2003).
[46] H. Kowalski, L. Motyka, and G. Watt, hep-ph/0606272.
[47] D. Muller, hep-ph/0605013.
[48] A. Airapetian *et al.* (HERMES Collaboration), Phys. Rev. Lett. **87**, 182001 (2001).
[49] B. Seitz (HERMES Collaboration), Nucl. Phys. **A721**, 785 (2003).
[50] F. Ellinghaus (HERMES Collaboration), Nucl. Phys. **A711**, 171 (2002).
[51] F. Ellinghaus, Report No. DESY-THESIS-2004-005.
[52] B. Krauss (HERMES Collaboration), hep-ex/0505016.
[53] Z. Ye (HERMES Collaboration), Proc. Sci., HEP2005 (2006) 120.
[54] Z. Ye, hep-ex/0606061.
[55] HERMES Collaboration, hep-ex/0605108.
[56] A. Bacchetta, U. D'Alesio, M. Diehl, and C. A. Millet, Phys. Rev. D **70**, 117504 (2004).
[57] F. Ellinghaus, W. D. Nowak, A. V. Vinnikov, and Z. Ye, hep-ph/0506264.
[58] S. Stepanyan *et al.* (CLAS Collaboration), Phys. Rev. Lett. **87**, 182002 (2001).